Three-Dimensional Computerized Tomographic Reconstruction of Instantaneous Distribution of Chemiluminescence of a Turbulent Premixed Flame*

Yojiro ISHINO** and Norio OHIWA**

The advanced CT (computerized tomography) reconstruction technique for measuring an instantaneous three-dimensional distribution of chemiluminescence of a turbulent premixed flame is accomplished. In the technique, first, instantaneous two-dimensional images ('projection' images) of an objective flame are simultaneously taken from forty horizontal directions with a forty-lens camera. Next four hundred horizontal CT images, which are reconstructed from the 'projection' images by MLEM (maximum likelihood expectation maximization) algorithm, are vertically accumulated, resulting in an instantaneous three-dimensional distribution of flame-chemiluminescence. Results for a propane-air fuel-rich-premixed turbulent flame are as follows. The flame front is observed to be a thin wrinkled luminous region of 0.6 mm in thickness. The three-dimensional result clearly shows that the cusps observed in horizontal cross-sections correspond to ridges of the three-dimensional flame front. The luminosity is quenched at the ridges by Lewis number effect. Finally, various types of display of three-dimensional distribution are performed to demonstrate the three-dimensionality of data acquisition.

Key Words: Digital Image Processing, Flow Visualization, Turbulent Flow, Combustion, Extinction, Flame, Optical Measurement, Three-Dimensional Measurement, Computerized Tomography

1. Introduction

Many experimental and computational studies have been made on the flame structure in turbulent premixed flames[(1)–(11)]. During the last decade, two-dimensional laser diagnostic techniques, such as particle image velocimetry (PIV) and planar laser induced fluorescence (PLIF) technique, have progressively been employed to investigate flame extinction mechanisms in turbulent flames [(12)–(19)] and in the interacting flames with vortices[(20)–(24)]. Recently three-dimensional measurement is strongly required for detail investigation of behavior of turbulent flame, since three-dimensional turbulent flame front structures are difficult to analyze from planar measurements solely. Therefore a variety of multi-plane experiments has been conducted. Bingham et al.[(25)] utilized the crossed-plane laser sheet for conventional tomographic measurement of a turbulent V-flame. Chen and Mansor [(26)] and O'Young and Bilger[(27)] obtained data of a two-plane two-dimensional Rayleigh thermometry of a turbulent flame using a couple of laser light sheets. Moreover, Dinkelacker et al.[(28)] reported simultaneous two-plane two-dimensional OH and temperature measurements for locally quenched highly turbulent lean premixed flames. In addition, Landenfeld et al.[(29)] measured two-dimensional distributions of temperature and OH concentration in three adjacent planes (distance 1 mm) with two excimer lasers and six image-intensified charge-coupled device (CCD) cameras. Although much effort to obtain the three-dimensional information have been paid in the multi-plane, so-called 'three-dimensional' experiments, the thickness of measured volume is considerably restricted owing to complex arrangements of diagnostic systems and their expensive costs.

In order to elucidate detail three-dimensional structure of turbulent flame, it is worth obtaining the whole shape of instantaneous reaction zone of turbulent flame. In present study, therefore, another approach, that is,

* Received 23rd April, 2004 (No. 04-4097)

** Graduate School of Engineering, Nagoya Institute of Technology, Gokiso-cho, Showa-ku, Nagoya 466–8555, Japan. E-mail: ishino@nitech.ac.jp

instantaneous three-dimensional emission CT (computerized tomography) technique is proposed and accomplished for a turbulent propane-air fuel-rich premixed flame. First instantaneous two-dimensional images ('projection' images) of an objective flame are simultaneously taken from forty horizontal directions with a custom-made multi-lens camera, which has forty lenses and a roll of film. Next four hundred horizontal CT images, which are reconstructed from the 'projection' images by MLEM (maximum likelihood expectation maximization)-CT algorithm[30)–32)], are vertically accumulated, resulting in an instantaneous three-dimensional distribution of flame-chemiluminescence. The results for a propane-air fuel-rich-premixed turbulent flame show that the flame front is observed to be a thin wrinkled luminous region of 0.6 mm in thickness and that the cusps observed in horizontal cross-sections correspond to ridges of the three-dimensional flame front. It is found that the luminosity distribution is quenched along the ridges by Lewis number effect.

Tomographic reconstruction techniques, which based on transmission or emission techniques, have been utilized in combustion studies. Transmission tomographic reconstruction has been widely used[33)–39)]. Correia et al.[40)] made a comparison between transmission and emission tomographic reconstruction techniques, and mentioned that the disadvantage of transmission technique lay in the need for background light source. Two-dimensional emission reconstruction of temperature has been made by Leipertz et al.[41)] Time averaged three-dimensional emission reconstruction of temperature, which is based on the radiation from luminous flame, has been attempted by Correia et al.[40)] Most of emission techniques have been applied to the measurement of local flame temperature fields[40)]. Applications of emission tomography for internal engine diagnostic system have been reported by Phillip et al.[42)], however, the reconstructed images were ambiguous in order to investigate the turbulent flame front structure.

Inferring heat release rate or fuel consumption rate from chemiluminescence (e.g. C_2^* and CH^*. Here the * denotes an electronically excited state)[43)–48)] has long been a common and largely accepted practice. In this proposed technique, the chemiluminescence light emitted from premixed flame is focused. However Najm et al.[49)] and Rehm and Paul[50)] warn recently that such a chemiluminescence is not universally correlated with heat release rate and is not adequate indicators of local extinction of flame surface. Najm et al.[49)] found that the mole fraction of HCO had excellent correlation with heat release rate over the whole range of unsteady curvature and strain-rate investigated in their study. Rehm and Paul[50)] proposed the usage of the product of CO and OH-LIF signals as a marker of local heat release rate or dilatation rate in flame front. Three-dimensional tomographic reconstruction of weak LIF signal seems impossible at present because of difficulty in volumetric laser excitation and lack of sensitivity of cameras. As alternative way, chemiluminescence from premixed flame is selected for present investigation.

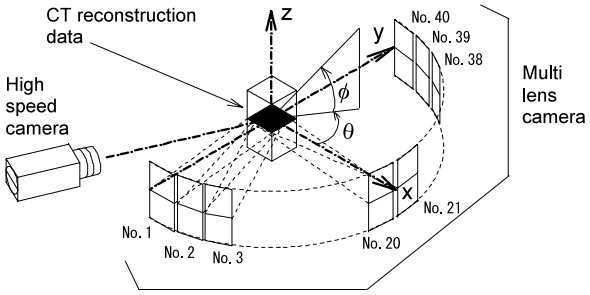

Fig. 1 Schematic diagram of the experimental apparatus and coordinates system

2. Experimental Apparatus and Method

2.1 Instantaneous 3D-CT method

The schematic diagram of the experimental apparatus and coordinates system is shown in Fig. 1. The cartesian $x-y-z$ coordinate and polar $\theta-\phi$ coordinate system are also depicted in the figure. In this method, first, the pipe burner with a turbulent premixed flame is settled at the center of a custom-made multi-lens camera, which has forty lenses no.1 – no.40. Instantaneous two-dimensional 'projection' images (no.1 – no.40) of chemiluminescence of an objective flame are simultaneously taken from forty directions using the multi-lens camera. This simultaneous photographic technique is called as 'time-slice' photography. By use of MLEM-CT algorithm, instantaneous two-dimensional chemiluminescence distributions of each horizontal cross-sections are reconstructed from related sets of forty horizontal line data picked up from 'projection' images. Instantaneous three-dimensional distribution is simply built up by accumulating vertically the numerous horizontal two-dimensional CT reconstructions. The objective turbulent flame is also monitored simultaneously by high speed CCD camera from the reverse direction of lens no.33.

2.2 'Time-slice' photographic technique

2.2.1 Multi-lens camera For 'time-slice' photography, a custom-made camera is designed. Figure 2 shows the dimensions of the camera, and the appearance and close-up of the camera are shown in Fig. 3. The camera is equipped with forty small high-performance lenses (6 elements/5 group, focal length f = 30 mm, F number=3.0, non-permeability to ultraviolet light). This semi-circular-arc shape of the camera can surround the objective flame over 180 degree for proper CT reconstruction. Very high-speed black and white negative panchromatic film (Fuji, Neopan 1 600. sensitivity is up to 630 nm) is loaded along the circumference of the camera, and developed after exposure. A free-falling slit shutter (5 mm in

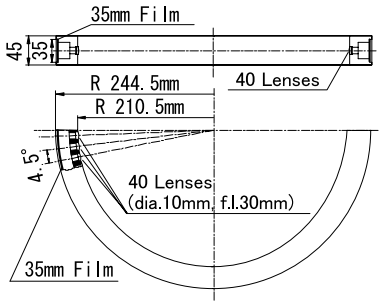

Fig. 2 Dimensions of custom-made multi-lens camera

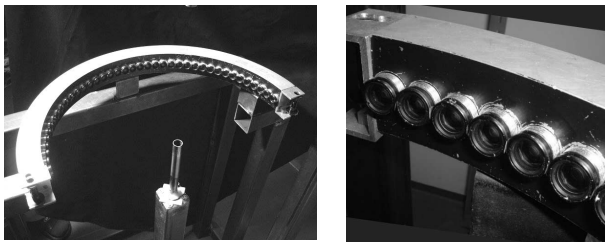

Fig. 3 Appearance (left) and close-up (right) of multi-lens camera which equipped with forty small lenses

slit size), which travels simultaneously in front of every lens, controls exposure time of 1.2 ms. In this system, although no interference filter for radical emission is used in order to ensure the fast-shuttering, the detection wavelength is limited to 400 – 600 nm by combination of the panchromatic film and the non-UV lenses used. In this investigation, therefore, detected flame images are treated as those of chemiluminescence.

2.2.2 Digital image processing The developed negative film is digitized with a macro lens on a digital camera (Nikon, D1) to obtain the forty digital 'projection' images of a turbulent flame. Alignment of each 'projection' image is performed on the basis of burner rim position of each image. The pixel values of the digital images are still qualitative, because no compensation for the characteristic curve, which ensures the relation between exposure and density of negative film, has been made. In this experiment, however, the linear proportion between the pixel values and integrated emission intensity on the line of sight at the pixel is tentatively assumed.

2.3 CT reconstruction

2.3.1 MLEM algorithm[31] In present study, MLEM (maximum likelihood-expectation maximization) method[30)–(32)] is employed for CT reconstruction. This reconstruction method is a kind of iterative reconstruction methods. The iterative reconstruction has recently become be attractive as an alternative to conventional filtered back-projection algorithm[51], because of its quantitative capability. Figure 4 shows the notation and coordinate system for MLEM reconstruction. λ_j^k is the value of reconstructed image at the pixel j for k-th iteration, y_i the measured projection data at i-th pixel, and C_{ij} the detection probability

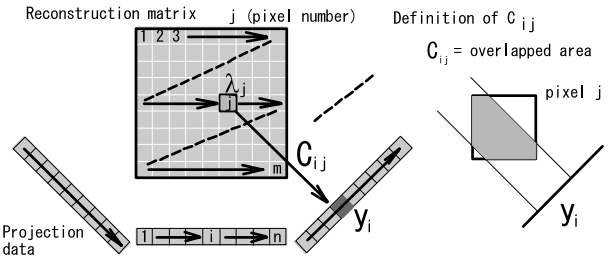

Fig. 4 Notation and coordinate system for MLEM reconstruction[31]

which represents as the overlapped area between i-th ray and pixel j. In MLEM reconstruction, for improvement of reconstruction image λ_j, the iteration is progressed by following expression:

$$\lambda_j^{k+1} = \left(\lambda_j^k \Big/ \sum_j C_{ij} \right) \sum_i \left[y_i C_{ij} \Big/ \sum_{j'} \left(C_{ij'} \lambda_{j'}^k \right) \right] \qquad (1)$$

where k is the iteration number. This algorithm converge to the maximum likelihood estimate of a probability distribution function from the observed data[30),(31)].

In the reconstruction of present study, conventional back-projection image is progressed by eight MLEM iterative steps. The emission light is assumed to be parallel ray for simplification of calculation. This parallel-beam assumption can be made by assuming that the objective flame size is negligible compared to the distance between objective flame and lenses. Although inclusion of absorption term is possible in MLEM method, absorption is not considered in present investigation because the self-absorption at bands of CH, C_2 and HCO is very weak in small flames[52].

2.3.2 Data size The forty 'projection' images of 380 pixel (horizontal) × 550 pixel (vertical) produces 550 sheets of horizontal reconstructed image of 380 pixel×380 pixel. It takes approximately 12 hours with Pentium 4 (1.7 GHz clock speed) PC to complete the reconstruction of 550 images. The pixel size corresponds to 0.12 mm. Therefore, the spacial resolution in the three-dimensional distribution is 0.12 mm × 0.12 mm × 0.12 mm, in each direction. Such high special resolution requires many 'projection' images taken by 40 lenses.

2.4 High speed photography

A high speed CCD video camera (Redlake, MotionScope PCI 1000S, 500 fps) monitors the turbulent flame behavior before and after exposure of multi-lens camera from the reverse direction of no.33 lens of the multi-lens camera. A flash light inserts a time mark on high speed movie at the exposure of the multi-lens camera.

2.5 Objective flame

Turbulent flame of propane-air rich mixture is investigated in this study. The 1.7 m/s propane-air mixture flow of 1.43 of equivalence ratio, issues from a burner pipe of 14 mm in inner-diameter, 16 mm in outer-diameter and

750 mm in length. The vertical position of burner rim is set 20 mm below the axes of lenses of multi-lens camera. Turbulence intensity of 0.09 m/s is promoted by the grid located in the pipe, despite of low Reynolds number of 1 526. It is well known that dark ridges appeared along the flame surface of rich propane-air mixture[53].

3. Results and Discussion

3.1 Motion characteristics of objective flame

Result of high speed photography of 500 frame/s is indicated in Fig. 5. The upper-right picture with flash light corresponds to the image recorded by multi-lens camera. The numbers denoted in each picture represent the time after recording by multi-lens camera. The consecutive pictures of Fig. 5 show that the objective flame is unsteady turbulent flame. It is suggested by the picture of 0 ms that the instantaneous objective flame at recording by multi-lens camera inclines to x or $-y$ direction, taking the high speed camera direction into consideration.

3.2 'Projection' images taken by 'time-slice' photography

Figure 6 shows a sample set of 'projection' images taken by multi-lens camera. The characters indicate the lens numbers. These pictures show instantaneous shape of one turbulent flame observed in different directions. Each flame has dark area on the flame surface. No one can tell the position of the dark region. As mentioned above, propane rich premixed flame tends to open at ridge or flame tip[53] in itself, even if no turbulence exists. It is expected that the dark region lies on the ridge of flame. There is no evidence for it, until reconstructions are made.

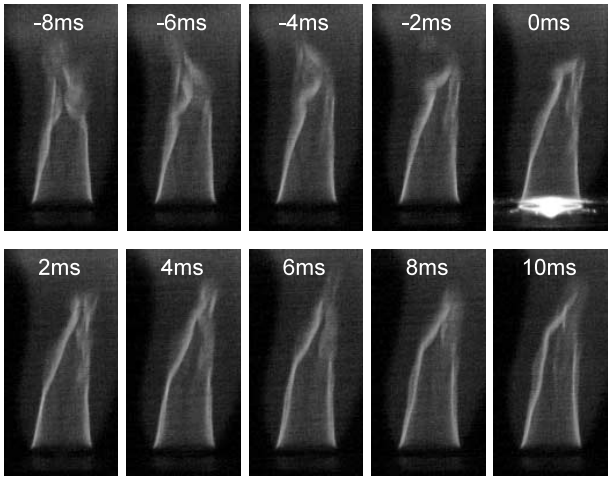

Fig. 5 High speed photography (500 frame/s). The upper-right picture with flash light corresponds to the image recorded by multi-lens camera.

3.3 Three-dimensional-CT reconstruction

Four hundred horizontal images are reconstructed from 'projection' images, and stacked up in order to make three-dimensional distribution. First, selected horizontal reconstructions are indicated in Fig. 7. For reference, A '$-x$ directional' virtual image shown in Fig. 8, which is made of the 3D distribution, gives the information of sections of each figure. Fig. 7 (a) – (i) correspond to the tomographic images of z = 36.0 mm, 32.4 mm, 28.8 mm, 25.2 mm, 21.6 mm, 18.0 mm, 14.4 mm, 10.8 mm and 7.2 mm in height from burner rim. Thin ring type distribution is observed at lower height (Fig. 7 (h) and (i)). In the middle region (Fig. 7 (d), (e) and (f)), it is found that frame front is folded, and the emission intensities are diminished at cusps, resulting from the so-called Lewis number effect. A set of horizontal reconstruction data proves that the 'cusps' in two-dimensional plane are ridges in three-dimensional space.

Next, in order to investigate the reconstruction accuracy, the data of z = 7.2 mm (Fig. 7 (i)) is examined in de-

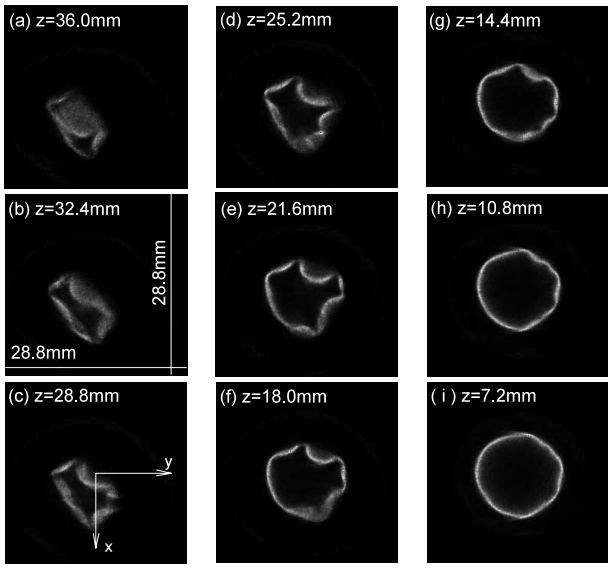

Fig. 7 Samples of horizontal reconstruction of turbulent premixed flame of propane-air rich mixture

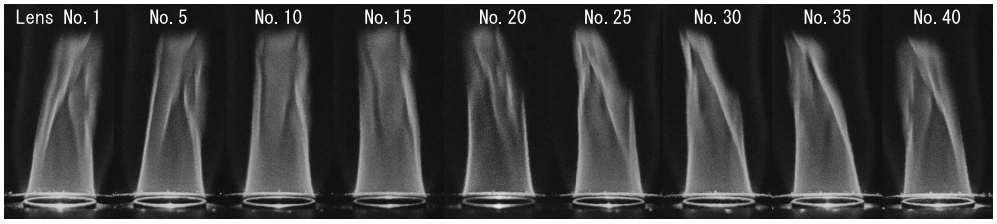

Fig. 6 Sample set of 'projection' images taken simultaneously by multi-lens camera

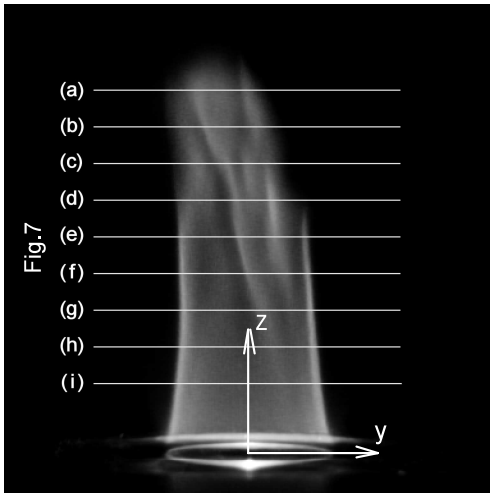

Fig. 8 A "$-x$ directional" virtual image made of the 3D distribution gives the information of sections for Fig. 7.

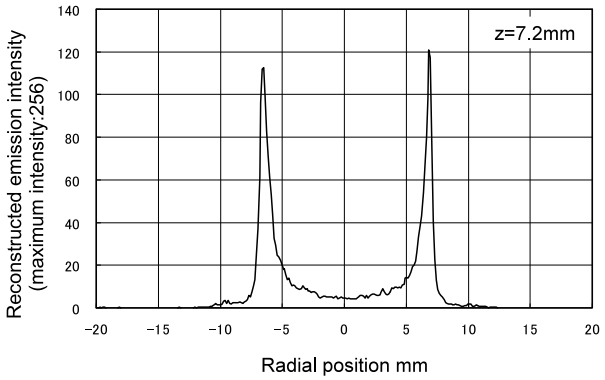

Fig. 9 Investigation of reconstruction accuracy based on the data of $z = 7.2$ mm (Fig. 7 (i)). The width (HWHM) of luminous region of reconstructed image is measured as 5 pixel (= 0.6 mm)

tail. Figure 9 shows the reconstructed intensity at the center line $x = 0$ mm. Half width at half maximum (HWHM) width of luminous region is measured as 5 pixel (approx.), that is 0.6 mm in width. Luminous region of turbulent premixed flames with weak turbulent intensity is considered to be thinner than pixel size 0.12 mm. This difference results from (i) long exposure time for fast movement, (ii) inaccuracy of CT reconstruction which concerns number of iteration, number of lenses, pixel size of images, parallel beam approximation, etc., (iii) no compensation in emission intensity data processing (especially, assumption of linear proportion between digitized pixel value and emission intensity), (iv) optical error (aberrations of lens, halation on film, etc.), etc.

Figure 10 displays the various types of observation of three-dimensional emission intensity distribution data set. It should be noted that artificial gradation is applied on Fig. 10. Figure 10 (a) and (b) are bird's eye views in directions of (θ,ϕ) = (60 deg, 30 deg) and (60 deg, 60 deg), respectively. Figure 10 (c) indicates a vertical sectional

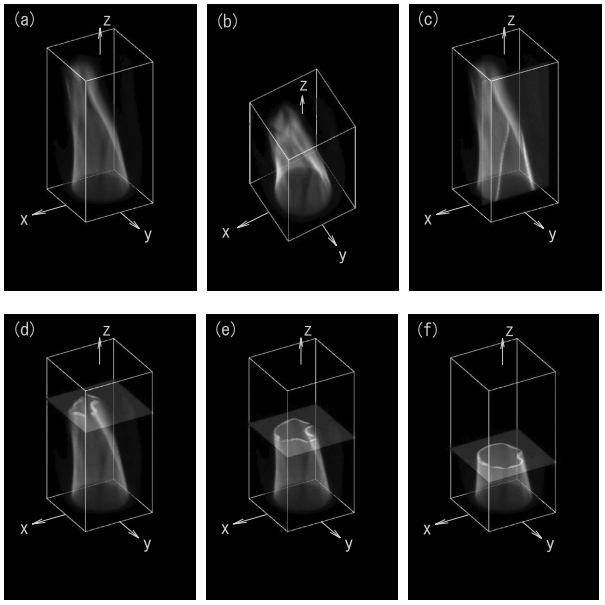

Fig. 10 Various types of display of three-dimensional emission intensity distribution data set. Artificial gradation is applied. Figure (a) and (b) : bird's eye views in directions of (θ,ϕ) = (60 deg, 30 deg) and (60 deg, 60 deg), (c) : vertical (y = 4.8 mm) sectional view, (d), (e) and (f) are horizontal sectional views at z = 28.8 mm, 21.6 mm, and 14.4 mm.

view. Figure 10 (d), (e) and (f) are horizontal sectional views at deferent vertical position z=28.8 mm, 21.6 mm, and 14.4 mm. These displays help us to recognize the detail and total shape of objective flame.

4. Conclusions

In present study, the advanced CT (computerized tomography) reconstruction technique for measuring an instantaneous three-dimensional distribution of chemiluminescence of a turbulent premixed flame is accomplished for a turbulent propane-air rich premixed flame. First, instantaneous two-dimensional chemiluminescence images of a turbulent premixed flame is simultaneously captured from forty directions using custom-made multi-lens camera, which has forty lenses. Next instantaneous three-dimensional emission distribution was reconstructed from the set of two-dimensional 'projection' images by use of MLEM-CT algorithm.

Four hundred horizontal images are reconstructed from 'projection' images, and accumulated vertically in order to make three-dimensional distribution. Thin ring type distribution of luminous region is observed at lower height of objective flame. In the middle height region, it is found that flame front is folded, and the emission intensities are diminished at cusps, resulting from the so-called Lewis number effect. A set of horizontal reconstruction data proves that the 'cusps' in two-dimensional plane are ridges in three-dimensional space. The width of

luminous region in a reconstructed image is measured as 5 pixel (= 0.6 mm), which is considerably thicker than that of luminous region of turbulent premixed flames. Various types of display of three-dimensional emission intensity distribution data set are performed, for example, bird's eye views, a vertical sectional view, and horizontal sectional views. These displays help us to recognize the detail and total shape of objective flame. It is, however, suggested that ample room of improvement still lay on this system, for example, (i) exposure time, (ii) CT reconstruction accuracy and (iii) quantitative evaluation between digitized pixel value for chemiluminescence intensity, etc.

Acknowledgments

The authors gratefully acknowledge Mr. Daiji OKAMOTO, Mr. Takeshi FUJI, and Mr. Osamu INAGAWA for their contribution during this experiment.

References

(1) Louch, D.S. and Bray, K.G., Vorticity and Scalar Transport in Premixed Turbulent Combustion, Proc. Combust. Inst., Vol.27 (1998), pp.801–810.

(2) Chen, J.H. and Im, H.G., Correlation of Flame Speed with Stretch in Turbulent Premixed Methane/Air Flames, Proc. Combust. Inst., Vol.27 (1998), pp.819–826.

(3) Sinibaldi, J.O., Mueller, C.J. and Driscoll, J.F., Local Flame Propagation Speed along Wrinkled, Unsteady, Stretched Premixed Flames, Proc. Combust. Inst., Vol.27 (1998), pp.827–832.

(4) Peters, N., Terhoeven, P., Chen, J.H. and Echekki, T., Statistics of Flame Displacement Speeds from Computations of 2-D Unsteady Methane-Air Flames, Proc. Combust. Inst., Vol.27 (1998), pp.833–839.

(5) Patnaik, G. and Kailasanath, K., A Computational Study of Local Quenching in Flame-Vortex Interactions with Radiative Losses, Proc. Combust. Inst., Vol.27 (1998), pp.711–717.

(6) Katta, V.R., Hsu, K.Y. and Roquemore, W.M., Local Extinction in an Unsteady Methane-Air Jet Diffusion Flame, Proc. Combust. Inst., Vol.27 (1998), pp.1121–1129.

(7) Chen, J.H. and Im, H.G., Stretch Effects on the Burning Velocity of Turbulent Premixed Hydrogen/Air Flames, Proc. Combust. Inst., Vol.28 (2000), pp.211–218.

(8) Knio, O.M. and Najm, H.N., Effect of Stoichiometry and Strain Rate on Transient Flame Response, Proc. Combust. Inst., Vol.28 (2000), pp.1851–1857.

(9) Bell, J.B., Brown, N.J., Day, M.S., Frenklach, M., Grcar, J.F. and Tonse, S.R., The Dependence of Chemistry on the Inlet Equivalence Ratio in Vortex-Flame Interactions, Proc. Combust. Inst., Vol.28 (2000), pp.1933–1939.

(10) Finke, H. and Grunefeld, G., An Experimental Investigation of Extinction of Curved Laminar Hydrogen Diffusion Flames, Proc. Combust. Inst., Vol.28 (2000), pp.2133–2140.

(11) Hasselbrink, E.F., Jr. and Mungal, M.G., Characteristics of the Velocity Field near the Instantaneous Base of Lifted Non-Premixed Turbulent Jet Flames, Proc. Combust. Inst., Vol.27 (1998), pp.867–873.

(12) Mansor, M.S., Peters, N. and Chen, Y.C., Investigation of Scalar Mixing in the Thin Reaction Zones Regime Using a Simultaneous CH-LIF/Rayleigh Laser Technique, Proc. Combust. Inst., Vol.27 (1998), pp.767–773.

(13) Renou, B., Boukhalfa, A., Puechberty, D. and Trinite, M., Effects of Streach on the Local Structure of Freely Propagating Premixed Low-Turbulent Flames with Various Lewis Numbers, Proc. Combust. Inst., Vol.27 (1998), pp.841–847.

(14) Masri, A.R., Kelman, J.B. and Dally, B.B., The Instantaneous Spatial Structure of the Recirculation Zone in Bluff-Body Stabilized Flames, Proc. Combust. Inst., Vol.27 (1998), pp.1031–1038.

(15) Rehm, J.E. and Clemens, N.T., The Relationship between Vorticity/Strain and Reaction Zone Structure in Turbulent Non-Premixed Jet Flames, Proc. Combust. Inst., Vol.27 (1998), pp.1113–1120.

(16) Han, D. and Mungal, M.G., Simultaneous Measurement of Velocity and CH Layer Distribution in Turbulent Non-Premixed Flames, Proc. Combust. Inst., Vol.28 (2000), pp.261–267.

(17) Bockle, S., Kazenwadel, J., Kunzelmann, T., Shin, D.I., Schulz, C. and Wolfrum, J., Simultaneous Single-Shot Laser-Based Imaging of Formaldehyde, OH, and Temperature in Turbulent Flames, Proc. Combust. Inst., Vol.28 (2000), pp.279–286.

(18) Burkert, A., Grebner, D., Muller, D., Triebel, W. and Konig, J., Single-Shot Imaging of Formaldehyde in Hydrocarbon Flames by XeF Excimer Laser-Induced Fluorescence, Proc. Combust. Inst., Vol.28 (2000), pp.1655–1661.

(19) Ishino, Y., Hasegawa, T., Yamaguchi, S. and Ohiwa, N., Optical Analysis of Pulse Combsution Using Shadowgraph and Planar CH-LIF Imaging Technique, Trans. A.S.M.E., J. Energy Resources Technol., Vol.123 (2001), pp.59–63.

(20) Katta, V.R., Carter, C.D., Fiechtner, G.J., Roquemore, W.M., Gord, J.R. and Rolon, J.C., Interaction of a Vortex with a Flat Flame Formed between Opposing Jets of Hydrogen and Air, Proc. Combust. Inst., Vol.27 (1998), pp.587–594.

(21) Yoshida, K. and Takagi, T., Transient Local Extinction and Reignition Behavior of Diffusion Flames Affected by Flame Curvature and Preferential Diffusion, Proc. Combust. Inst., Vol.27 (1998), pp.685–692.

(22) Mueller, C.J. and Schefer, R.W., Coupling of Diffusion Flame Structure to an Unsteady Vortical Flow-Field, Proc. Combust. Inst., Vol.27 (1998), pp.1105–1112.

(23) Thevenin, D., Renard, P.H., Fiechtner, G.J., Gord, J.R. and Rolon, J.C., Regimes of Non-Premixed Flame-Vortex Interactions, Proc. Combust. Inst., Vol.28 (2000), pp.2101–2108.

(24) Santoro, V.S., Kyritsis, D.C., Linan, A. and Gomez, A., Vortex-Induced Extinction Behaivior in Methanol Gaseous Flames: A Comparison with Quasi-Steady Extinction, Proc. Combust. Inst., Vol.28 (2000), pp.2109–

2116.
(25) Bingham, D.C., Gouldin, F.C. and Knaus, D.A., Crossed-Plane Laser Tomography: Direct Measurement of the Flamelet Surface Normal, Proc. Combust. Inst., Vol.27 (1998), pp.77–84.
(26) Chen, Y.C. and Mansour, M.S., Investigation of Flame Broadening in Turbulent Premixed Flames in the Thin-Reaction-Zones Regime, Proc. Combust. Inst., Vol.27 (1998), pp.811–818.
(27) O'Young, F. and Bilger, R.W., Scalar Gradient and Related Quantities in Turbulent Premixed Flames, Combust. Flame, Vol.109 (1997), pp.682–700.
(28) Dinkelacker, F., Soika, A., Most, D., Hofmann, D., Leipertz, A., Polifke, W. and Dobbeling, K., Structure of Locally Quenched Highly Turbulent Lean Premixed Flames, Proc. Combust. Inst., Vol.27 (1998), pp.857–865.
(29) Landenfeld, T., Kremer, A., Hassel, E., Janicka, J., Schafer, T., Kazenwadel, J., Schulz, C. and Wolfrum, J., Laser-Diagnostic and Numerical Study of Strongly Swirling Natural Gas Flames, Proc. Combust. Inst., Vol.27 (1998), pp.1023–1029.
(30) Dempster, A.P., Laird, N.M. and Rubin, D.B., Maximum-Likelihood from Incomplete Data via the EM Algorithm, J. Royal Statist Soc., B, Vol.39 (1977), pp.1–38.
(31) Yokoi, T., Shinohara, H., Hashimoto, T., Yamamoto, T. and Niio, Y., Implementation and Performance Evaluation of Iterative Reconstruction Algorithms in SPECT: A Simulation Study Using EGS4, Proc. the Second Int. Workshop on EGS, KEK Proceedings 200-20, (2000), pp.224–234.
(32) Tang, H.R., Da Silva, A.J., Matthay, K.K., Price, D.C., Huberty, J.P., Hawkins, R.A. and Hasegawa, B.H., Neuroblastoma Imaging Using a Combined CT Scanner-Scintillation Camera and ^{131}I-MIBG, J. Nuclear Medicine, Vol.42, No.2 (2001), pp.237–247.
(33) Ray, S. and Semerjian, H., In Combustion Diagnostics by Non-Intrusive Methods, Edited by McCay, T. and Roux, V., (1984), p.92, AIAA, New York.
(34) Hall, R. and Bonczyk, P., Sooting Flame Thermometry Using Emission/Absorption Tomography, Appl. Opt., Vol.29, No.31 (1990), pp.4590–4598.
(35) Burkhardt, H. and Stoll, E., Edited by Williams, R.A. and Beck, M.S., In Process Tomography, (1995), Butterworth-Heinemann, Oxford, U.K.
(36) Shimizu, S., Sakai, S. and Wakai, K., Simultaneous Measurement of Temperature and Density of Burnt Gases by an Infrared Radiation Computed Tomography, Heat Transfer in Radiating and Comb. Systems, (1992), pp.309–331, Springer Verlag.
(37) Shimizu, S. and Sakai, S., High-Speed Tomography for Simultaneous Measurement of the Histories of Two-Dimensional Distributions of Temperature and Density of Burnt Gases, JSME Int. J., Ser. B, Vol.37, No.3 (1994), pp.596–603.
(38) Hertz, H.M., Experimental Determination of 2-D Flame Temperature Fields by Interferometric Tomography, Opt. Commun. Vol.54, No.3 (1985), pp.131–136.
(39) Sato, S. and Kumakura, T., Interferometric Tomography Measurement of Temperature Fields in Turbulent Flame, Joint Int. Conf. AUS/NZ and JS/CI, (1989), pp.195–197.
(40) Correia, D.P., Ferrao, P. and Caldeire-Pires, A., Flame Three-Dimensional Tomography Sensor for In-Furnace Diagnostics, Proc. Combust. Inst., Vol.28 (2000), pp.431–438.
(41) Leipertz, A., Obertacke, R. and Wintrich, F., Industrial Combustion Control Using Transmission Tomography, Proc. Combust. Inst., Vol.26 (1996), pp.2869–2875.
(42) Phillip, H., Hirsch, A., Baumgartner, M., Fernitz, G., Beidl, C., Piock, W. and Winklhoger, E., Localization of Knock Events in Direct Injection Gasoline Engines, SAE paper, No.2001-01-1199 (2001).
(43) Hurle, I.R., Price, R.B., Sugden, F.R.S. and Thomas, A., Sound Emission from Open Turbulent Premixed Flames, Proc. Roy. Soc., A, Vol.303 (1968), pp.409–427.
(44) Ducruix, S., Durox, D. and Candel, S., Theoretical and Experimental Determinations of the Transfer Function of a Laminar Premixed Flame, Proc. Combust. Inst., Vol.28 (2000), pp.765–773.
(45) Ishino, Y., Kojima, T., Oiwa, N. and Yamaguchi, S., Phase Characteristics of Coherent Structure in Acoustic Excited Plane Diffusion Flames, Ninth Symp. (Int.) on Turbulent Shear Flows, No.31-1 (1993), pp.1–6.
(46) Ishino, Y., Kojima, T., Oiwa, N. and Yamaguchi, S., Acoustic Excitation of Diffusion Flames with Coherent Structure in a Plane Shear Layer (Application of Active Combustion Control to Two-Dimensional Phase-Locked Averaging Measurement, JSME Int. J., Ser. B, Vol.39, No.1 (1996), pp.156–163.
(47) Kojima, J., Ikeda, Y. and Nakajima, T., Spatially Resolved Measurement of OH^*, CH^*, and C_2^* Chemiluminescence in the Reaction Zone of Laminar Methane/Air Premixed Flames, Proc. Combust. Inst., Vol.28 (2000), pp.1757–1764.
(48) Ikeda, Y., Kojima, J., Nakajima, T., Akamatsu, F. and Katsuki, M., Measurement of the Local Flame-front Structure of Turbulent Premixed Flames by Local Chemiluminescence, Proc. Combust. Inst., Vol.28 (2000), pp.343–350.
(49) Najm, H.N., Paul, P.H., Mueller, C.J. and Wyckoff, P.S., On the Adequacy of Certain Experimental Observables as Measurements of Flame Burning Rate, Combust. Flame, Vol.113 (1998), pp.312–332.
(50) Rehm, J.E. and Paul, P.H., Reaction Rate Imaging, Proc. Combust. Inst., Vol.28 (2000), pp.1775–1782.
(51) Herman, G.T., Image Reconstruction from Projections, (1980), p.118, Academic Press, New York.
(52) Gaydon, A.G., The spectroscopy of Flames, (1974), p.12, Chapman and Hall, London, U.K.
(53) Lewis, B. and von Elbe, G., Combustion, Flames and Explosions of Gases, (1961), p.309, Academic Press, New York.